

# Effect of Vertical or Beveled Chondral Defect Creation on Rim Deformation and Contact

CARTILAGE

1–7

© The Author(s) 2018

Reprints and permissions:

[sagepub.com/journalsPermissions.nav](http://sagepub.com/journalsPermissions.nav)

DOI: 10.1177/1947603517752058

[journals.sagepub.com/home/CAR](http://journals.sagepub.com/home/CAR)

Adam B. Yanke<sup>1</sup>, Megan L. Konopka<sup>1</sup>, Davietta C. Butty<sup>1</sup>, Maximilian A. Meyer<sup>1</sup>, Eric J. Cotter<sup>1</sup>, Alejandro A. Espinoza<sup>1</sup>, and Brian J. Cole<sup>1</sup>

## Abstract

**Objective.** To determine biomechanical effects of knee cartilage defect perimeter morphology based on cartilage strain and opposing subchondral bone contact. **Design.** Articular cartilage defects were created in 5 bovine femoral condyles: group 1, 45° inner bevel with 8-mm rim; group 2, vertical with 8-mm rim; and group 3, 45° outer bevel with 8-mm base. Samples were placed into a custom-machined micro-computed tomography tube and subjected to 800 N of axial loading. DICOM data were used to calculate cartilage thickness 4 and 6 mm from the center, distance between tibial cartilage surface and femoral subchondral bone, and contact width between tibial cartilage and subchondral bone. Strain 4 mm from the center and both absolute and change in distance (mm) to subchondral bone were compared between groups 1 and 2 using paired *t* tests. Strain at 6 mm and distance changed, loaded distance, and contact width (mm) were compared between groups using the Friedman test with *post hoc* analysis using Wilcoxon signed rank test. **Results.** No significant differences in rim strain were noted between groups 1 and 2 at 4 mm ( $P = 0.10$ ) and between groups 1, 2, and 3 at 6 mm ( $P = 0.247$ ) from the defect center. The loaded distance was significantly different between groups 1 and 3 ( $P = 0.013$ ). No significant change in distance to the subchondral bone was found between groups ( $P = 0.156$ ). The difference in subchondral bone contact area approached but did not reach significance ( $P = 0.074$ ). **Conclusion.** When debriding focal articular cartilage defects, establishment of an inner bevel decreases tissue deformation and contact with opposing subchondral bone.

## Keywords

articular cartilage, debridement, perimeter morphology, bevel

## Introduction

Cartilage defects of the knee cause a significant burden to both the patient by generating pain and society by expediting progression of osteoarthritis. It is estimated that approximately 63% of individuals undergoing arthroscopy have articular cartilage defects.<sup>1</sup> Much of this is due to the inability of cartilage to restore its native structure.<sup>2</sup> While treatments continue to evolve, ranging from simple debridement to cell-based surface treatments, the first step of nearly every cartilage restoration procedure remains preparation of a stable vertical wall at the periphery of the defect.<sup>3,4</sup> Survey data suggests that 97% of surgeons debride cartilage back to a stable layer while performing microfracture.<sup>5</sup> While this is likely advantageous in the setting of microfracture, it is unclear if it is beneficial to perform the procedure in a similar manner when performing debridement alone.

Nearly 3 decades ago, the veterinary community explored the effect of peripheral wall morphology in the

debridement of articular cartilage defects and concluded that beveled walls may lead to cartilage defect size progression.<sup>6</sup> However, the beveling process in this study necessarily enlarged the defects and therefore clouded accurate assessment of disease progression. This point has not undergone further discussion, and the assumption remains that vertical walls are superior. Clinically, cartilage defects are still commonly debrided as part of a staging arthroscopy or as the first stage of a 2-stage restoration. Yet it remains unclear if debridement to a vertical wall yields biomechanical advantages, such as decreased compressive ability or reduced subchondral bone contact, in comparison

<sup>1</sup>Department of Orthopaedic Surgery, Rush University Medical Center, Chicago, IL, USA

### Corresponding Author:

Brian J. Cole, Department of Orthopaedic Surgery, Rush University Medical Center, 1611 West Harrison Street, Suite 300, Chicago, IL 60611, USA.

Email: [bcole@rushortho.com](mailto:bcole@rushortho.com)

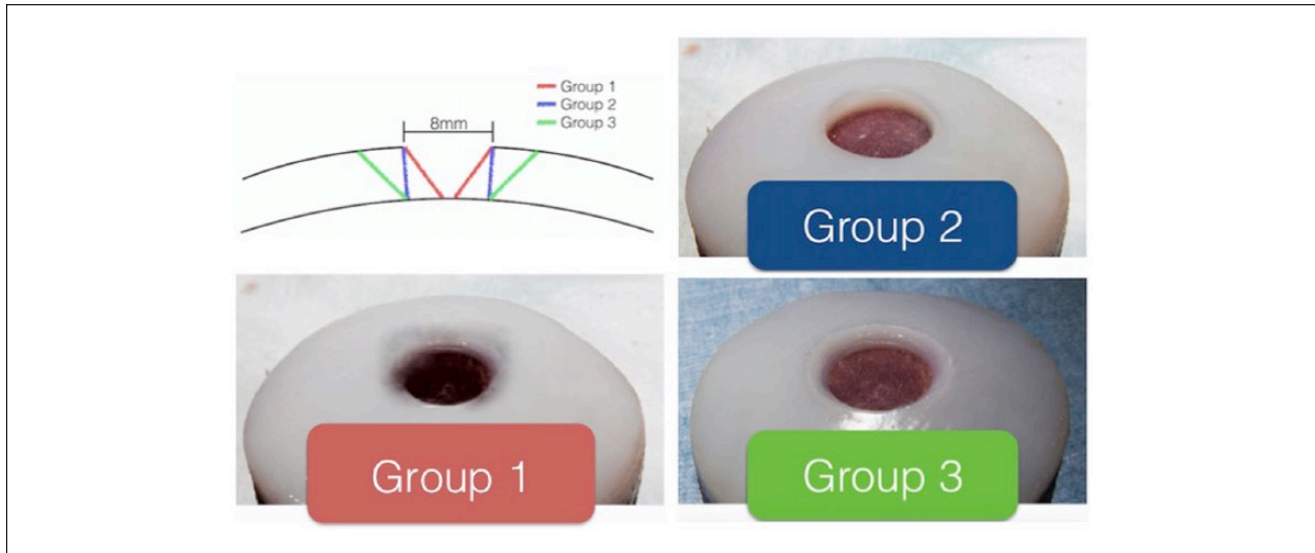


**Figure 1.** Illustration of the 3 medial femoral condyle defects evaluated in this study. [AQ: 3]

to an inner or outer bevel. The purpose of this study was to determine the local biomechanical effects of cartilage defect perimeter morphology based on cartilage strain and contact with opposing subchondral bone. The authors hypothesized that increasing the surface diameter of a cartilage defect would increase opposing contact with subchondral bone and that vertical walls would have greater strain resistance than beveled walls.

## Methods

### Sample Preparation and Defect Creation

Bovine knees ( $n = 5$ ) were harvested and the articular surface of the medial femoral condyle was exposed. The knee was placed in a vice and Kirschner wires were passed across the joint to maintain native congruity. The center of the medial femoral condyle was harvested using a 30-mm coring reamer, taking care to remain perpendicular to the articular surface. A corresponding core of articular cartilage of the tibial plateau was harvested using the same process. After this was complete, full-thickness cartilage defects were created in the femoral condyle according to the following groups: (1) inner bevel with 8 mm rim, (2) vertical with 8-mm rim, and (3) outer bevel with 8-mm base (**Fig. 1**). These were created sequentially by starting with a 2-mm skin biopsy punch. For group 1, this was followed by creation of a 45° beveled defect with a custom-machined device, resulting in a 8-mm rim at the chondral surface. This was followed by an 8-mm skin biopsy punch to progress to group 2. In a similar fashion to group 1, a second custom-machined device was used to create 45° beveled walls with an inner base diameter of 8 mm.

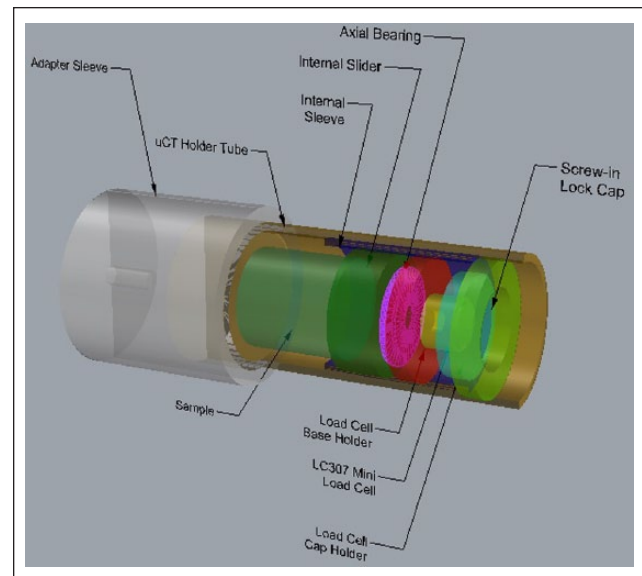


**Figure 2.** Illustration of a custom-machined micro-computed tomography ( $\mu$ CT) tube that allows for controlled axial loading.

### Sample Testing and Imaging

To prepare the samples for computed tomography (CT) imaging, the femoral plug was stained overnight at 4°C with 40% Hexabrix ioxaglate radiological contrast (Guerbet, Roissy, France) and 60% 0.15 M phosphate buffered saline (PBS), which renders articular cartilage surfaces distinguishable by micro-CT. After removing excess solution with gauze, the samples were loaded in apposition to approximate anatomical orientation into a custom-machined micro-CT tube that allowed for controlled axial loading (**Fig. 2**). To limit variability, all samples were marked to ensure the same

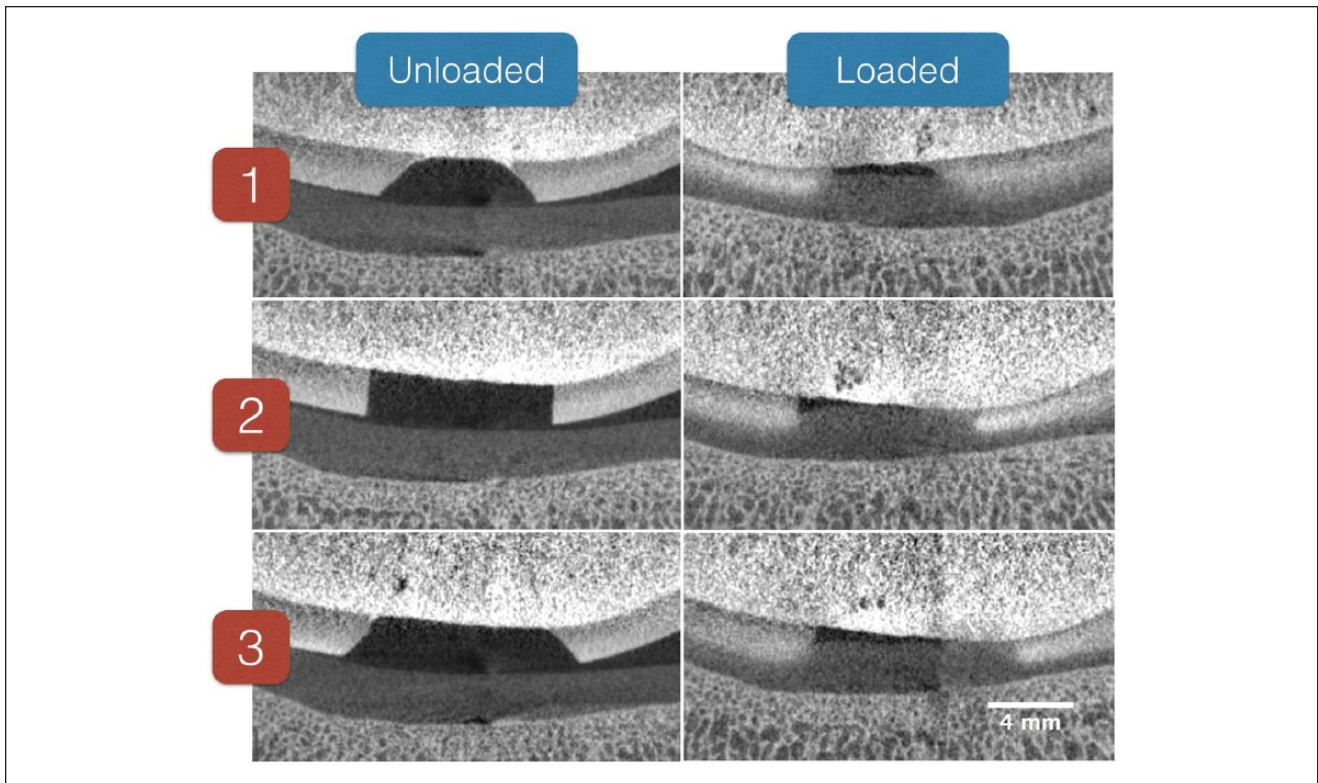


**Figure 3.** Micro-computed tomography ( $\mu$ CT) images of all defect groups both with and without axial loading.

orientation with each subsequent scan. For each sample and defect size, images were obtained in the micro-CT scanner (Scanco uCT 50, Bruettisellen, Switzerland) without and then with axial loading (**Fig. 3**). For all samples, micro-CT was set at—scanner,  $\mu$ CT40  $\mu$ CT50; voxel size, 40  $\mu$ m; x-ray tube potential (peak), 70 kVp; x-ray intensity, 114  $\mu$ A; integration time, 300 [AQ: 1]. The applied load was monitored through a miniature load cell placed inside the tube (Omega LC307-series 1000 N button load-cell, Omegadyne, Inc., Sunbury, OH). The sample was loaded to 800 N using this method. The loaded sample was allowed to relax and equilibrate over the course of 10 minutes, with measurements of decremental load dissipation occurring each minute prior to being introduced to the micro-CT scanner. Scan time was approximately 45 minutes per sample. All testing for a given sample was done without any freeze-thaw cycles in between and completed on the same day.

### Data Collection and Analysis

Raw DICOM (Digital Imaging and Communications in Medicine) data from the micro-CT scanner was imported into OsiriX (Pixmeo SARL, 2003-2014). Using 3-dimensional (3D) orthogonal reconstructions, sample images were reoriented to the same plane using anatomic landmarks to ensure the same view was analyzed for all groups.

Using the coronal reconstructions, the following data were obtained for the loaded and unloaded samples in all groups: cartilage thickness 4 and 6 mm from the center, minimum distance of tibial cartilage surface to the center of exposed femoral subchondral bone, and, if contacting, the width of the contact of the cartilage on the bone. Whenever possible, measurement was made at the center of the defect and checked using 3D reconstructions to minimize variability.

Using descriptive statistics (average and standard deviation), the strain applied at 4 and 6 mm from the center was calculated. These peripheral defect measurements were taken at the same respective location on both sides of each defect type within a sample. Strain was calculated using the equation  $\varepsilon = [(d - d_0)/d_0] \times 100$ . The absolute length and change in distance to the subchondral bone was also calculated (**Fig. 4**). Using paired *t* tests, strain at 4 mm was compared between group 1 and group 2. Strain at 6 mm was compared between all groups using first a repeated-measures 1-way analysis of variance; however, the data proved to have an outlier value, so a Friedman test was used given the nonparametric nature of the data. The amount of 2D contact and distance (mm) to the subchondral bone was also compared between all groups using a Friedman test. Significance for all tests was set at  $P < 0.05$ . Statistical calculations were carried out using the SPSS 18.0 (SPSS, Chicago, IL, USA).

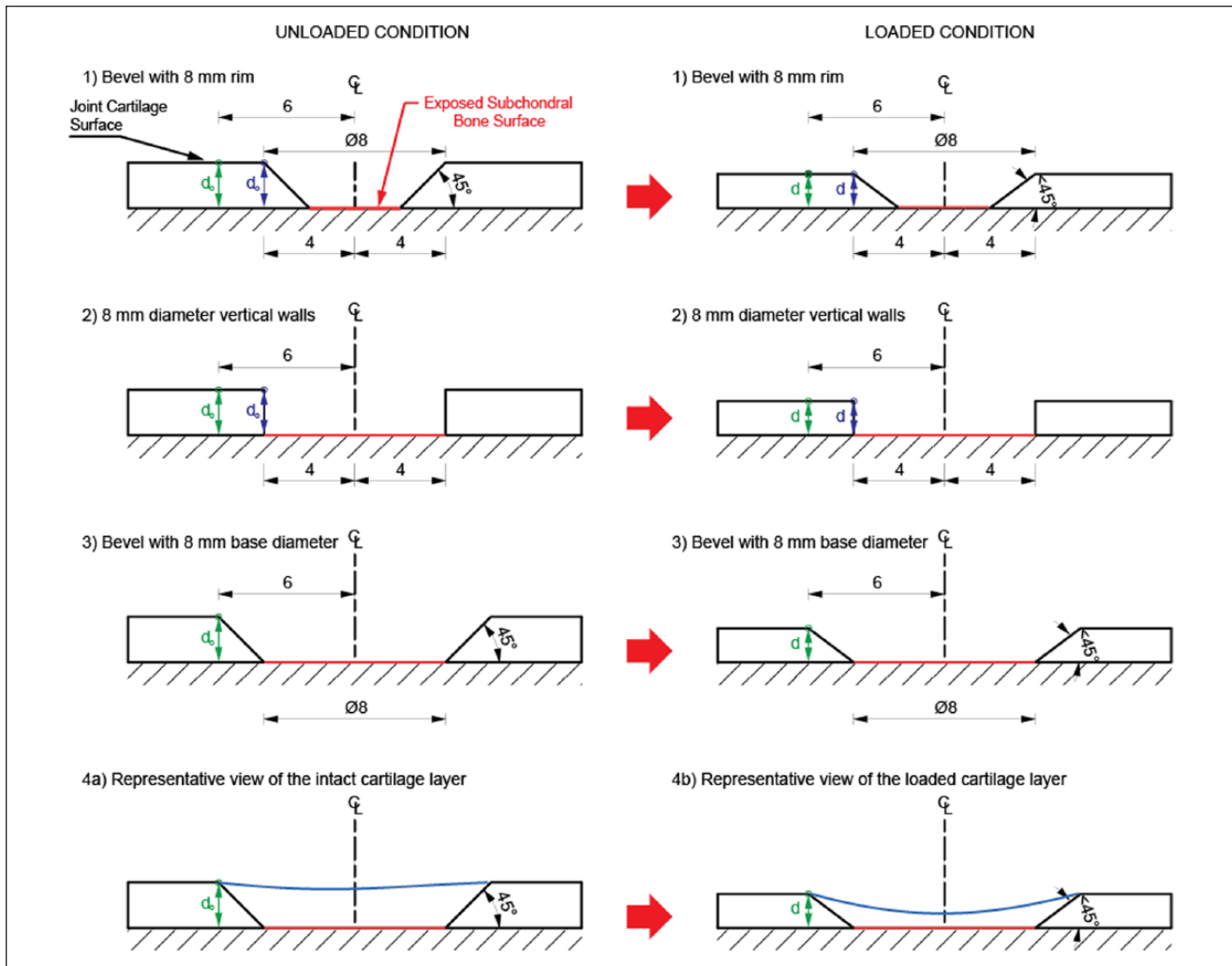


**Figure 4.** Schematic of measurements taken. In all cases,  $d_0$  and  $d$  correspond to distances measured in the unloaded and loaded conditions, respectively. Given that the subchondral layer is exposed,  $d_0$  and  $d$  also equal the distance to subchondral bone in the unloaded and loaded conditions, respectively, when measured from the center of the defect. The 4 mm radius measurements are shown in blue, and the 6 mm measurements are shown in green. In all cases, strain is calculated as  $\varepsilon = [(d - d_0)/d_0] \times 100$  to show the strain at the wall height, with  $d$  always smaller than  $d_0$ . Note that the bevel angle decreases below  $45^\circ$  after the load is applied in groups 1 and 3. Measurement of cartilage wall height at 4 mm radius is not possible for group 3 because that material has already been removed by the bevel.

## Results

Rim strain did not change significantly within groups when moving from 4 to 6 mm from the center of the defect. When comparing rim strain at 4 and 6 mm, there were no significant differences between groups (4 mm,  $0.61 \pm 0.10$  and  $0.50 \pm 0.16$  for groups 1 and 2, respectively; 6 mm,  $0.54 \pm 0.11$ ,  $0.47 \pm 0.17$ , and  $0.64 \pm 0.17$  for Groups 1, 2, and 3, respectively;  $P > 0.05$ ) (Table 1). On axial loading, a significant difference was shown between group 1 ( $0.82 \pm 0.33$ ), group 2 ( $0.50 \pm 0.41$ ), and group 3 ( $36 \pm 0.44$ ) ( $P = 0.015$ ). On *post hoc* analysis using Wilcoxon signed rank test, group 1 exhibited a significantly greater loaded distance compared

**Table 1.** Differences in Rim Strain Between Groups.

Group	4-mm Strain	6-mm Strain
1	$0.61 \pm 0.10$	$0.54 \pm 0.11$
2	$0.50 \pm 0.16$	$0.47 \pm 0.17$
3	Not applicable	$0.64 \pm 0.17$
<i>P</i>	0.10	0.247

with group 3, that is, changing the wall profile from inner bevel to outer bevel ( $P = 0.013$ ) (Table 2). No significant differences were noted between group in the minimum distance of tibial cartilage surface to the center of exposed

**Table 2.** Differences in Distance to Subchondral Bone Between Groups.

	Group 1	Group 2	Group 3	P
Loaded distance (mm)	0.82 ± 0.33	0.50 ± 0.41	0.36 ± 0.44	0.015 <sup>a</sup>
Distance change (mm)	-1.09 ± 0.21	-1.49 ± 0.19	-1.41 ± 0.33	0.156
Contact (mm)	0 ± 0	0.8 ± 1.6	3.2 ± 3.9	0.074

<sup>a</sup>Group 1 versus group 3 had a *P* value = 0.013 in *post hoc* analysis using Wilcoxon signed rank test.

femoral subchondral bone. Group 1 defects did not display any contact with opposing subchondral bone. However, no significant difference was noted in the amount of opposing subchondral bone contact area between groups.

## Discussion

This study resulted from the basic assumption that, just as a car tire traveling over a pothole may experience different amounts of deformation based on the size and morphology of the hole, similar effects may be noticed with cartilage defects (Fig. 5). Specifically, the increased surface diameter may be more predictive of deformation and contact of the healthy cartilage with the opposing subchondral bone. The findings of this study suggest that keeping an inner bevel of tissue may decrease tissue contact with the opposing subchondral bone. Proposed clinical consequences of preserving subchondral bone from contact and subsequent sclerosis include decreased pain after debridement, as articular cartilage is aneural, as well as improved success rates for downstream cartilage restoration strategies, such as autologous chondrocyte implantation.<sup>7,8</sup> Further human studies are needed to determine the extent to which contact with subchondral bone affects pain and functional outcomes.

While not significant, there was a trend toward the ability of vertical walls to shield the neighboring tissue from strain. Prior work has demonstrated that there is a critical defect size at which rim stress increases significantly. Brown *et al.*<sup>9</sup> demonstrated that the “critical strain size” for canine models is 2 mm. Similarly, Guettler *et al.*<sup>10</sup> demonstrated no change in surrounding peak stress in human knees until defects were >8 mm in diameter, with a 64% increase in 10-mm defects. Interestingly, there was no increased peak stress when moving from 10- to 20-mm defects. Our study therefore chose to evaluate an inner and outer bevel from this 8-mm critical value since bovine knees are similar to human knees in overall size. However, while moving from group 2 to group 3 increased the lesion surface radius from 4 to 6 mm, there was no significant change in strain at 6 mm. This suggests that at this size there was no effect of protecting the cartilage from deformation, while it did decrease the amount of deformation on the contralateral surface.

The results of this study are revealing when evaluated in the setting of the work by Rudd *et al.*<sup>6</sup> Specifically, while

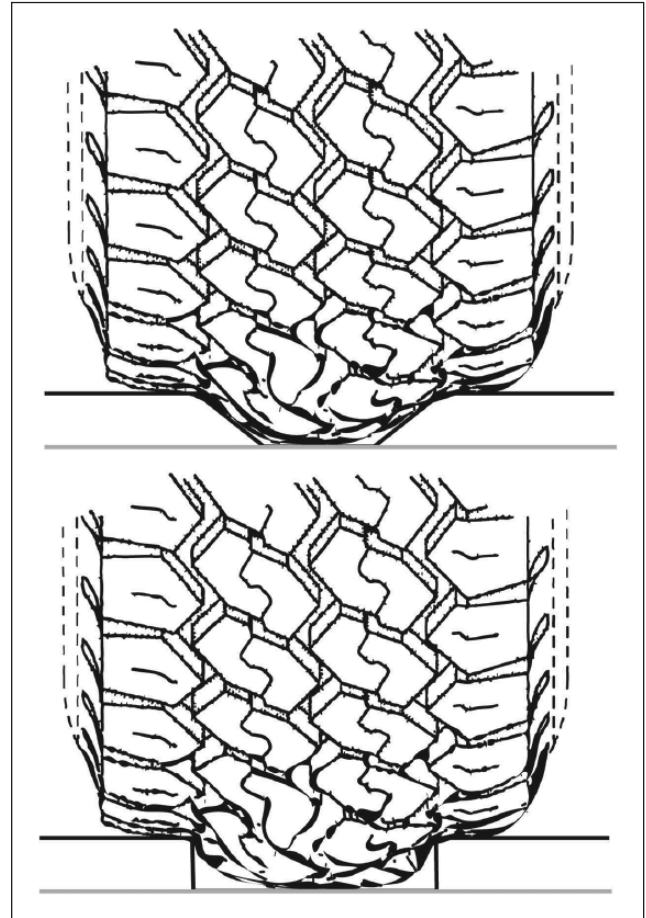


**Figure 5.** Deformation of a car tire depends largely on the size and shape of the pothole that it passes over. Similarly, debridement of cartilage defects to either beveled (top) or vertical (bottom) walls may alter biomechanical properties such as deformation, strain, and contact with subchondral bone.

the authors did not see defect size progression with beveling defects, they reported increased erosion on the surface opposing the beveled defects. The authors attribute this finding to be more related to the overall superficial diameter of the defect than to the morphology of the rim itself. In this light, this is why there was more effect on strain when moving from group 2 to 3 as opposed to moving from group 1 to 2. Beveling may also have the effect of increased sliding strain magnitudes as compared to nonbeveled defects.<sup>11</sup>

## Limitations

This study has several limitations, including the limitations of any *in vitro* analysis. This study is limited with regard to the variability in the bovine knee contour and specific location of the defect. While each statistical comparison was made within the same knee, there is still increased variability that is imposed on the system due to these differences. However, the authors still felt that this model is more clinically relevant than a pure finite element analysis simulation without this variability. Furthermore, in order to create 3 distinct groups, the beveling process necessarily removed differing amounts of tissue for each group, which may confound interpretation of local strain results. However, in order to analyze 3 potential debridement strategies for a roughly 8-mm defect in a clinically relevant fashion, such differences in volume removed were considered unavoidable. While all attempts were made to apply uniform loading, it was not possible to monitor this during the scanning procedure. Also, the tissue used was healthy and therefore the properties of degenerative tissue left at the base of the defect may not be represented. This property has been described by Nelson *et al.*<sup>12</sup> where they demonstrated no difference in rim stress in fresh canine defects and in those filled with fibrocartilage. Finally, the methods employed with  $\mu$ CT are novel and provide different information than pressure sensors that have shown to have an error ranging from 11.7% to 20%.<sup>13</sup>

## Conclusion

Though this study could not evaluate degenerative tissue, the findings suggest that the establishment of an inner bevel in the treatment of articular cartilage defects in the knee provides unique biomechanical advantages, namely decreasing tissue deformation and subsequent contact with opposing subchondral bone. Clinical studies are needed to determine if these advantages translate to clinically relevant decreases in patient pain after debridement. As expected, there does not appear to be a role for an outer bevel into healthy adjacent cartilage tissue.

## Acknowledgments and Funding

The research was conducted at Rush University Medical Center. The study was internally funded.

## Declaration of Conflicting Interests

The author(s) declared the following potential conflicts of interest with respect to the research, authorship, and/or publication of this article: ABY reports research support from Anthrax, Inc. and NuTech Medical and serves as a paid consultant for JRF Ortho. BJC reports the following disclosures: Aesculap/B.Braun, research support; *American Journal of Orthopedics*, editorial or governing board; American Orthopaedic Society for Sports Medicine, board

or committee member; American Shoulder and Elbow Surgeons, board or committee member; Arthrex, Inc., intellectual property royalties, paid consultant, research support; *Arthroscopy*, editorial or governing board; Arthroscopy Association of North America, board or committee member; Athletico, other financial or material support; Cytori, research support; Elsevier Publishing, intellectual property royalties; International Cartilage Repair Society, board or committee member; *Journal of Bone and Joint Surgery–American*, editor; *Journal of Shoulder and Elbow Surgery*, editor; *Journal of the American Academy of Orthopaedic Surgeons*, editor; National Institutes of Health (NIAMS and NICHD), research support; Ossur, other financial or material support; Regentis, paid consultant, stock or stock options; Saunders/Mosby-Elsevier, publishing royalties, financial or material support; Smith & Nephew, other financial or material support; Tornier, other financial or material support.

## Ethical Approval

Ethical approval for this study was obtained from \*NAME OF ETHICS COMMITTEE OR INSTITUTIONAL REVIEW BOARD (APPROVAL NUMBER/ID)\*. **[AQ: 2]**

**Or**

Ethical approval for this study was waived by \*NAME OF ETHICS COMMITTEE OR INSTITUTIONAL REVIEW BOARD\* because \*REASON FOR WAIVER\*.

**Or**

Ethical approval was not sought for the present study because \*REASON\*.

## Animal Welfare

The present study followed international, national, and/or institutional guidelines for humane animal treatment and complied with relevant legislation.

**Or**

The present study involved client-owned animals; it demonstrated a high standard (best practice) of veterinary care and involved informed client consent.

**Or**

Guidelines for humane animal treatment did not apply to the present study because \*REASON\*.

## References

1. Curl WW, Krome J, Gordon ES, Rushing J, Smith BP, Poehling GG. Cartilage injuries: a review of 31,516 knee arthroscopies. *Arthroscopy*. 1997;13(4):456-60.
2. Hunter W. Of the structure and disease of articulating cartilages. *Philos Trans R Soc Lond B Biol Sci*. 1743;42B:514-21.
3. Riboh JC, Cole BJ, Farr J. Particulated articular cartilage for symptomatic chondral defects of the knee. *Curr Rev Musculoskelet Med*. 2015;8(4):429-35.
4. Pascual-Garrido C, McNickle AG, Cole BJ. Surgical treatment options for osteochondritis dissecans of the knee. *Sports Health*. 2009;1(4):326-34.
5. Theodoropoulos J, Dwyer T, Whelan D, Marks P, Hurtig M, Sharma P. Microfracture for knee chondral defects: a survey of surgical practice among Canadian orthopedic surgeons. *Knee Surg Sports Traumatol Arthrosc*. 2012;20(12):2430-7.

6. Rudd RG, Visco DM, Kincaid SA, Cantwell HD. The effects of beveling the margins of articular cartilage defects in immature dogs. *Vet Surg.* 1987;16(5):378-83.
7. Minas T, Gomoll AH, Rosenberger R, Royce RO, Bryant T. Increased failure rate of autologous chondrocyte implantation after previous treatment with marrow stimulation techniques. *Am J Sports Med.* 2009;37(5):902-8.
8. Flanigan DC, Harris JD, Brockmeier PM, Siston RA. The effects of lesion size and location on subchondral bone contact in experimental knee articular cartilage defects in a bovine model. *Arthroscopy* 2010;26(12):1655-61.
9. Brown TD, Pope DF, Hale JE, Buckwalter JA, Brand RA. Effects of osteochondral defect size on cartilage contact stress. *J Orthop Res.* 1991;9(4):559-67.
10. Guettler JH, Demetropoulos CK, Yang KH, Jurist KA. Osteochondral defects in the human knee: influence of defect size on cartilage rim stress and load redistribution to surrounding cartilage. *Am J Sports Med.* 2004;32(6):1451-8.
11. Gratz KR, Wong BL, Bae WC, Sah RL. The effects of focal articular defects on cartilage contact mechanics. *J Orthop Res.* 2009;27(5):584-92.
12. Nelson BH, Anderson DD, Brand RA, Brown TD. Effect of osteochondral defects on articular cartilage. Contact pressures studied in dog knees. *Acta Orthop Scand.* 1988;59(5):574-9.
13. Drewniak EI, Crisco JJ, Spenciner DB, Fleming BC. Accuracy of circular contact area measurements with thin-film pressure sensors. *J Biomech.* 2007;40(11):2569-72.